(49) R. S. Drago and T. C. Kuechler, Abstracts, 174th National Meeting of the American Chemical Society, Chicago, Ill., Aug. 1977, No. INOR-28.
(50) D. S. Martin, G. A. Robins, and P. E. Fanwick, Abstracts, 176th National Meeting of the American Chemical Society, Miami Beach, Fla., Sept. 1978, No. INOR-156.
(51) The only reported structure of a dirhodium tetraformate is of the monoaquo adduct,[52] and the only available details are given in a review article[53] as follows: Rh–Rh, 2.38 Å; Rh–$OH_2$, 2.20 Å; Rh–O (formate) axial, 2.45 Å; Rh–O (formate) equatorial, 2.03 Å. It is an *asymmetric* structure. Hopefully, a combination of new structural work (on the tetraformates) and calculations (on the tetraacetates) will lead to a resolution of the disagreements on the specific ordering of the levels.
(52) A. S. Antsyshkina, *Acta Crystallogr.*, **21**, A140 (1966); an abstract describing space group and cell constants for several tetraacetate structures is found on this page, work by L. M. Dikareva. This is obviously a misreference by the reviewer.
(53) E. M. Shustorovich, M. A. Porai-koshits, and Y. A. Buslaev *Coord. Chem. Rev.*, **17**, 1–98 (1975).
(54) P. H. Krupenie, *Natl. Stand. Ref. Data Ser., Natl. Bur. Stand.*, No. 5 (1966).
(55) Y. B. Koh and G. G. Christoph, *Inorg. Chem., in press.*
(56) (a) R. E. Rundle, *J. Phys. Chem.*, **61**, 45–50 (1957). (b) A recent excellent calculational example of the same concept is given by P. K. Mehrotra and R. Hoffmann, *Inorg. Chem.*, 17, 2187–2189 (1978).
(57) D. E. Williams, G. Wohlauer, and R. E. Rundle, *J. Am. Chem. Soc.*, **81**, 755–761 (1959); E. Frasson, C. Panattoni, and R. Zannetti, *Acta Crystallogr.*, **12**, 1027–1034 (1959).
(58) K. W. Browall, T. Bursh, L. V. Interrante, and J. S. Kasper, *Inorg. Chem.*, **11**, 1800–1806 (1972).
(59) F. Bonati and G. Wilkinson, *J. Chem. Soc.*, 3156–3162 (1964); F. Bonati and R. Ugo, *Chim. Ind. (Milan)* **46**, 1332–1334 (1964); N. A. Bailey, E. Coates, G. B. Robertson, F. Bonati, and R. Ugo, *Chem. Commun.*, 1041–1042 (1967); C. G. Pitt, L. K. Monteith, L. F. Ballard, J. P. Collman, J. C. Morrow, W. R. Roper, and D. Ulku, *J. Am. Chem. Soc.*, **88**, 4286–4287 (1966); K. Mann, N. S. Lewis, R. M. Williams, H. B. Gray, and J. G. Gordon, II, *Inorg. Chem.*, 17, 828–834 (1978); T. W. Thomas and A. E. Underhill *Chem. Soc. Rev.*, **1**, 99–120 (1972).
(60) A. L. Balch, *J. Am. Chem. Soc.*, **98**, 8049–8054 (1976); A. L. Balch and B. Tulyathan, *Inorg. Chem.*, **16**, 2840–2845 (1977); G. C. Gordon, P. W. DeHaven, M. C. Weiss, and V. L. Goedken, *J. Am. Chem. Soc.*, **100**, 1003–1005 (1978).
(61) J. C. Dewan, J. Silver, J. D. Donaldson, and M. J. K. Thomas, *J. Chem. Soc., Dalton Trans.*, 2315–2319 (1977).
(62) M. Corbett and B. F. Hoskins, *Chem. Commun.*, 1602–1604 (1968).
(63) J. Catterick, M. B. Hursthouse, P. Thornton, and A. J. Welch, *J. Chem. Soc., Dalton Trans.*, 223–226 (1977).

# Solid State Structure, Magnetic Susceptibility, and Single Crystal ESR Properties of *cis*-Diammineplatinum α-Pyridone Blue

**Jacqueline K. Barton,[1a,2] David J. Szalda,[1a] Harold N. Rabinowitz,[1a] Joseph V. Waszczak,[1b] and Stephen J. Lippard* [1a]**

*Contribution from the Department of Chemistry, Columbia University, New York, New York 10027, and Bell Laboratories, Murray Hill, New Jersey 07974.*
*Received August 13, 1978*

**Abstract:** The crystal and molecular structure and magnetic and ESR properties of *cis*-diammineplatinum α-pyridone blue are reported. The compound, a mixed valent tetramer having the formula $[(NH_3)_4Pt_2(C_5H_4NO)_2]_2(NO_3)_5 \cdot H_2O$, crystallizes in the triclinic system, space group $P\bar{1}$. The lattice parameters are $a$ = 10.219 (7) Å, $b$ = 11.225 (7) Å, $c$ = 9.538 (6) Å, $\alpha$ = 106.32 (2)°, $\beta$ = 93.91 (2)°, and $\gamma$ = 73.75 (2)°. The structure was solved using 4421 independent reflections collected on a four-circle X-ray diffractometer and refined to final values of the residuals $R_1 = 0.045$ and $R_2 = 0.058$. There is one cation per unit cell, consisting of two *cis*-diammineplatinum units bridged by two α-pyridonate ligands, and two of these are further linked across a crystallographic inversion center to form a tetranuclear chain. The platinum atoms at the ends of the chain are bonded to two ammine ligands in a cis configuration and two deprotonated nitrogen atoms of the α-pyridonate rings. The inner platinum atoms have two cis ammine groups and two exocyclic α-pyridonate ring oxygen atoms in their coordination spheres. Apart from the bridging α-pyridonate ligands, the two square planar platinum moieties are further joined by a Pt–Pt bond of 2.7745 (4) Å. The linkage of two of these binuclear units across the center of symmetry is achieved by a Pt–Pt bond, 2.8770 (5) Å in length, and by intramolecular hydrogen bonds formed between the ammines coordinated to one platinum atom and the coordinated oxygen atoms of its inversion mate. As a result of nonbonded steric interactions, the $Pt_4$ chain is not quite linear, with the Pt1–Pt2–Pt2′ angle being 164.60 (2)°. The Pt–O and Pt–N bond lengths range from 2.016 (8) to 2.041 (7) Å. There are, additionally, five nitrate anions and one water molecule in the unit cell. The average formal platinum oxidation state is therefore 2.25. Magnetic susceptibility measurements of the solid over the range 4.2 K < $T$ < 300 K show *cis*-diammineplatinum α-pyridone blue to be a simple Curie paramagnet. The magnetic moment of 1.81 $\mu_B$ is consistent with the presence of one unpaired spin per tetrameric unit. Single-crystal electron spin resonance measurements revealed the principal $g$ values to be $g_{xx}$ = 2.307, $g_{yy}$ = 2.455, and $g_{zz}$ = 1.975. The magnitudes and orientations of the **g** tensor components indicate that the unpaired spin resides in a molecular orbital comprised of $d_{z^2}$ atomic orbitals directed approximately along the platinum chain axis.

Blue platinum complexes have long been of interest to chemists.[3-6] In 1908 a blue compound was reported to form in a reaction between dichlorobis(acetonitrile)platinum(II) and silver salts.[3] This "Platinblau" was formulated as the monomeric platinum(II) complex, $[(CH_3CONH)_2Pt] \cdot H_2O$. Later it was proposed, by analogy to other deeply colored platinum and ruthenium compounds, that platinum complexes having anomalous blue colors were polymeric with bridging amidate linkages.[4] The tendency for square-planar platinum complexes to stack at close distances with favorable metal–metal axial interactions was realized at about the same time.[5] When blue crystals of a material, formed in the reaction of trimethylacetamide and $[(CH_3CN)_2PtCl_2]$, were obtained,[6] it appeared that the structure of a platinum blue would at last be solved by X-ray diffraction. Unfortunately, the crystals were found to be a 7:2:1 mixture of two isomorphous, yellow, crystalline components and an amorphous, blue material. Based on extensive chemical and spectroscopic analyses, the blue component was formulated as a mononuclear platinum(IV) compound, $[(t\text{-}C_4H_9CONH)_2PtCl_2]$. The original "Platinblau" was assigned the analogous formula $[(CH_3CONH)_2Pt(OH)_2]$.[6]

More recently, following the discovery[7] that *cis*-dichlorodiammineplatinum(II) (DDP) is an antitumor drug, a blue

0002-7863/79/1501-1434$01.00/0 

color was observed on incubation of the hydrolysis products of *cis*-DDP with polyuracil.[8] Subsequent work[8-13] showed that blue platinum complexes could be prepared with pyrimidines, substituted pyrimidines, and an assortment of substituted amides as ligands. These platinum pyrimidine and amide blues were found to have a high index of antitumor activity with a lower associated nephrotoxicity than the parent complex, *cis*-DDP. Neither *trans*-DDP nor dichloroethylenediamineplatinum(II) hydrolysis products could be employed in the synthesis of blue platinum pyrimidine compounds. Studies of the sedimentation[12] and magnetic[9,13] properties of the platinum pyrimidine blues showed them to be polymeric and paramagnetic. A polymeric structure was also suggested by the results of a californium-252 plasma desorption mass spectroscopic study.[14]

The most reasonable geometric model emerging from work on the platinum pyrimidine blues was that of a chain of amidate bridged platinum atoms having, most likely, a nonintegral oxidation state in order to account for the paramagnetism. Efforts to determine unambiguously the structure were thwarted, however, by the failure to obtain a crystalline blue product and the general lack of reproducibility in the preparation of these complexes. The fact that only amorphous blue powders were obtained is understandable in view of the general difficulty of crystallizing pure material from mixtures of polymers with varying chain lengths and degrees of stability.

As briefly described in a preliminary report,[15] we have obtained a crystalline platinum blue using α-pyridone (**1**) as the amide ligand. The presence of only one heterocyclic nitrogen atom and one exocyclic oxygen atom in this pyrimidine (**2**)

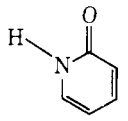

α-pyridone **1**

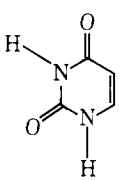

pyrimidine **2**

analogue permitted the isolation of crystalline material in which the extent of polymerization has been limited to four platinum units. Here we present the full details of the crystallographic determination as well as temperature-dependent magnetic susceptibility and single-crystal ESR results that define the molecular and electronic structures of *cis*-diammineplatinum α-pyridone blue in the solid state. Synthetic, redox, molecular weight, and electronic spectral studies of this and related platinum blues in solution will be described separately.[12]

## Experimental Procedure and Results

The synthesis of *cis*-diammineplatinum α-pyridone blue has been described elsewhere.[15,16]

**Collection and Reduction of X-ray Data.** Crystals from the original preparation of the compound were used to determine the lattice parameters and space group and for the solution and initial refinement of the structure.[15] Because the intensity of standard reflections decreased by 15% over the course of data collection, and since a modified preparative procedure[16] gave bigger crystals, a second data set was collected. Preliminary precession photographs showed the space group, $P1$ or $P\bar{1}$, and cell dimensions of the larger, higher quality crystals to be the same as those found previously. The crystal used for collecting the second data set was a parallelepiped of approximate dimensions 0.65 mm between (100) and ($\bar{1}$00) faces, 0.18 mm between (010) and (0$\bar{1}$0), 0.28 mm between (001) and (00$\bar{1}$), and with the (1$\bar{1}$1) face developed ~0.171 mm from the center. The crystal, still slightly wet with absolute ethanol used in the final wash,[15] was sealed in a Lindemann glass capillary. Crystal data and details of the data collection and reduction are given in Table I. The only significant difference between the lattice parameters in Table I and those reported previously[15] is the length of the *b* axis, which is 0.030 Å (~4σ) smaller and leads to correspondingly shorter bond distances.

**Table I.** Experimental Details of the X-ray Diffraction Study of *cis*-Diammineplatinum α-Pyridone Blue

A. Crystal Parameters at 23 °C[a]

| | |
|---|---|
| $a$ = 10.219 (7) Å | $V$ = 1008.0 Å$^3$ |
| $b$ = 11.225 (7) Å | mol wt = 405.3 for $[Pt(C_5H_4NO)(NH_3)_2](NO_3)_{1.25}(H_2O)_{0.25}$ |
| $c$ = 9.538 (6) Å | |
| $\alpha$ = 106.32 (2)° | space group $P\bar{1}$ |
| $\beta$ = 93.91 (2)° | $Z$ = 4 |
| $\gamma$ = 73.75 (2)° | $\rho$(obsd)[b] = 2.62 (2) g/cm$^3$ |
| | $\rho$(calcd) = 2.670 g/cm$^3$ |

B. Measurement of Intensity Data

instrument: Picker FACS-I-DOS diffractometer
radiation: Mo Kα ($\lambda_{\alpha_1}$ = 0.7093 Å), graphite monochromatized
takeoff angle: 2.0°
detector aperture: 6.33 × 6.33 mm
crystal-detector distance: 33 cm
scan technique: coupled $\theta$(crystal)-$2\theta$(counter)
scan range: 1.70° (symmetric, plus $K_{\alpha_1}$-$K_{\alpha_2}$ dispersion)
scan rate: 1.0°/min
maximum $2\theta$: 60°
background measurements: stationary crystal, stationary counter; 20-s counts at each end of $2\theta$ scan range
standards: three reflections ($\bar{5}12$), ($42\bar{4}$), and ($2\bar{3}1$) measured after every 97 reflections showed random, statistical fluctuations
no. of reflections collected: 5770 ($+h$, $\pm k$, $\pm l$)

C. Treatment of Intensity Data[c]

reduction to preliminary $F_o^2$ and $\sigma(F_o^2)$: correction for background, attenuators, and Lorentz-polarization of monochromatized X-radiation in the usual manner;[d] $\epsilon$[e] = 0.05. Owing to an adjustment of the electronics of the diffractometer, the intensities of the standard reflections increased by 10% for the data between 55° ≤ $2\theta$ ≤ 60°. A common factor was used to put these reflections on the same scale as the data having $2\theta$ < 55°.[f]
absorption correction: $\mu$ = 140.7 cm$^{-1}$. Transmission factors varied between 0.0295 and 0.1270.
observed data: 4421 unique reflections for which $F_o^2 > 3\sigma(F_o^2)$ were used in the refinement

[a] From a least-squares fit to the setting angles of 25 carefully centered reflections. [b] B suspension in $CHBr_3/CHCl_3$ mixtures. [c] Programs for an IBM 360/91 computer used in this work: UMAT, the local version of the Brookhaven diffractometer setting and cell constant and orientation refinement program; ORABS, the local version of the absorption correction program by D. J. Wehe, W. R. Busing, and H. A. Levy, adapted to FACS-I geometry; XDATA, the Brookhaven Wilson plot and scaling program; FOURIER, the Dellaca and Robinson modification of the Zalkin Fourier program FORDAP; CUGLS, the local version of the Busing-Martin-Levy structure factor calculation and least-squares refinement program (ORFLS) modified by Ibers and Doedens for rigid-body refinement; ORFFE, the Busing-Martin-Levy molecular geometry and error function program; ORTEP II, the Johnson thermal ellipsoid plotting program; in addition to various local data processing programs. [d] J. T. Gill and S. J. Lippard, *Inorg. Chem.*, **14**, 751 (1975). [e] P. W. R. Corfield, R. J. Doedens, and J. A. Ibers, *ibid.*, **6**, 197 (1967). [f] A. J. C. Wilson, *Nature (London)*, **150**, 151 (1942).

**Determination and Refinement of the Structure.** Using the original data set, the locations of the platinum atoms were derived from an unsharpened Patterson map. A structure factor calculation phased on four platinum atoms placed in an acentric cell, space group $P1$, gave a value of 0.191 for $R_1 = \Sigma||F_o| - |F_c||/\Sigma|F_o|$. A difference Fourier map revealed the C, N, and O atomic positions of the two ammines coordinated to each platinum atom and the four α-pyridonate ligands. At this stage the structure appeared to have an inversion center located between the two central platinum atoms. The atomic coordinates were therefore transformed to move the center of symmetry to the origin. The space group was thus assumed to be $P\bar{1}$, a choice that is justified by the successful refinement of the structure. Two subsequent difference Fourier calculations revealed the positions of 2.5 nitrate anions in the asymmetric unit, the "half-nitrate" being disordered about the

**Table II.** Final Positional and Thermal Parameters[a,b]

| ATOM | $x$ | $y$ | $z$ | $\beta_{11}$[c] | $\beta_{22}$ | $\beta_{33}$ | $\beta_{12}$ | $\beta_{13}$ | $\beta_{23}$ |
|---|---|---|---|---|---|---|---|---|---|
| Pt1 | 0.30929(3) | −0.31234(3) | −0.22811(3) | 5.96(4) | 4.43(3) | 6.94(4) | −1.00(2) | 0.42(2) | 1.41(2) |
| Pt2 | 0.09319(3) | −0.12130(3) | −0.07187(3) | 5.32(4) | 4.53(3) | 7.59(4) | −1.04(2) | 0.55(2) | 1.88(2) |
| O12 | 0.0800(6) | −0.0615(6) | −0.2548(6) | 6.3(7) | 5.4(5) | 9.1(7) | −0.4(5) | 1.3(5) | 2.4(5) |
| O22 | 0.2452(7) | −0.0400(6) | 0.0077(7) | 6.2(7) | 5.6(6) | 11.9(8) | −2.4(5) | −0.0(6) | 0.6(5) |
| N1 | 0.2118(9) | −0.4025(8) | −0.3978(9) | 9.4(10) | 7.1(8) | 9.7(9) | −3.3(7) | −1.9(7) | 1.7(7) |
| N2 | 0.3311(9) | −0.4616(7) | −0.1382(8) | 11.2(10) | 5.2(7) | 9.3(9) | −3.0(6) | −1.5(7) | 2.3(6) |
| N3 | −0.0632(8) | −0.1985(7) | −0.1477(9) | 4.9(8) | 4.9(6) | 14.7(12) | −1.6(5) | 0.7(7) | 0.2(7) |
| N4 | 0.1010(8) | −0.1787(7) | 0.1125(9) | 7.0(8) | 5.1(6) | 12.3(10) | 0.3(6) | 1.5(7) | 3.6(7) |
| N11 | 0.3001(8) | −0.1750(7) | −0.3320(7) | 8.2(8) | 5.3(6) | 7.4(7) | −4.1(6) | −0.6(6) | 1.0(5) |
| N21 | 0.4184(8) | −0.2263(7) | −0.0670(7) | 7.3(8) | 5.4(6) | 7.2(7) | −1.8(6) | −1.1(6) | 1.9(5) |
| C12 | 0.1869(9) | −0.0832(9) | −0.3386(9) | 7.2(9) | 6.7(8) | 7.5(9) | −2.3(7) | −0.6(7) | 1.9(7) |
| C13 | 0.1779(11) | −0.0044(9) | −0.4321(10) | 10.6(12) | 6.6(8) | 10.4(11) | −2.1(8) | −0.4(9) | 3.8(8) |
| C14 | 0.2872(13) | −0.0273(11) | −0.5207(11) | 15.8(16) | 9.1(11) | 9.8(11) | −5.3(11) | 1.2(11) | 4.2(9) |
| C15 | 0.4077(12) | −0.1218(11) | −0.5109(12) | 11.2(14) | 10.3(12) | 11.6(13) | −3.9(10) | 3.4(10) | 3.0(10) |
| C16 | 0.4109(11) | −0.1952(10) | −0.4163(11) | 8.6(11) | 6.8(9) | 11.0(11) | −2.2(8) | 2.9(9) | 0.7(8) |
| C22 | 0.3685(9) | −0.1064(8) | 0.0209(9) | 6.7(9) | 6.1(7) | 7.9(9) | −2.4(6) | 0.3(7) | 2.8(6) |
| C23 | 0.4511(10) | −0.0479(9) | 0.1309(9) | 8.6(11) | 7.0(8) | 8.2(9) | −3.5(7) | −0.1(8) | 1.0(7) |
| C24 | 0.5819(11) | −0.1156(11) | 0.1464(12) | 8.7(12) | 10.0(11) | 12.6(13) | −4.3(9) | −2.9(10) | 4.2(10) |
| C25 | 0.6340(11) | −0.2387(12) | 0.0521(12) | 7.0(11) | 10.9(12) | 13.6(14) | −2.4(9) | −2.2(9) | 5.5(11) |
| C26 | 0.5511(10) | −0.2895(9) | −0.0500(12) | 6.5(10) | 6.2(8) | 14.5(14) | −0.7(7) | −0.1(9) | 2.5(9) |
| O3 | 0.5946(10) | −0.5426(9) | −0.3451(9) | 17.8(14) | 11.3(10) | 11.9(10) | 2.1(10) | 1.5(10) | 3.5(8) |
| O4 | 0.6238(9) | −0.6425(8) | −0.1777(8) | 13.2(11) | 11.6(10) | 10.8(9) | −2.5(8) | 1.8(8) | 3.6(8) |
| O5 | 0.7847(10) | −0.6816(10) | −0.3316(9) | 13.3(12) | 15.3(13) | 13.5(11) | −2.0(10) | 0.9(9) | 6.6(10) |
| O6 | −0.0821(12) | −0.2605(13) | −0.4701(13) | 16.3(16) | 19.4(18) | 21.2(18) | −5.6(13) | −4.1(13) | 6.0(14) |
| O7 | −0.244(2) | −0.3205(15) | −0.6060(20) | 58(5) | 16.2(20) | 37(3) | −13(3) | −33(4) | 6(2) |
| O8 | −0.265(2) | −0.268(3) | −0.388(3) | 27(4) | 59(7) | 53(6) | −13(4) | −10(4) | 25(5) |
| O9 | 0.131(3) | −0.508(4) | 0.045(5) | 7(3) | 22(5) | 73(12) | −1(3) | 10(4) | −5(6) |
| O10 | −0.048(4) | −0.379(3) | 0.050(5) | 29(6) | 13(3) | 58(10) | −6(4) | −12(6) | 21(5) |
| O11 | −0.056(3) | −0.562(3) | 0.044(4) | 16(4) | 11(3) | 56(9) | −7(3) | 6(5) | 7(4) |
| N7 | 0.6691(10) | −0.6222(8) | −0.2856(8) | 11.8(12) | 6.9(8) | 8.5(9) | −1.3(7) | 0.0(8) | 0.8(7) |
| N8 | −0.194(2) | −0.2920(13) | −0.499(2) | 33(4) | 7.4(12) | 33(4) | −5.7(17) | −18(3) | 4.5(17) |
| N9 | 0.015(4) | −0.485(3) | 0.046(6) | 9(4) | 9(3) | 47(14) | −5(2) | 1(5) | 6(5) |
| OW1 | −0.021(3) | −0.484(3) | −0.293(4) | 24(5) | 15(3) | 39(6) | −10(3) | 5(4) | 6(4) |

[a] Atoms are labeled as indicated in Figure 1a. [b] Standard deviations, in parentheses, occur in the last significant figure for each parameter. [c] Anisotropic temperature factors (× $10^3$) are of the form $\exp[-(\beta_{11}h^2 + \beta_{22}k^2 + \beta_{33}l^2 + 2\beta_{12}hk + 2\beta_{13}hl + 2\beta_{23}kl)]$.

inversion center at (0, ½, 0). Several cycles of least-squares refinement were then carried out, minimizing the function $\Sigma w(|F_o| - |F_c|)^2$ where $w = 4F_o^2/\sigma^2(F_o)$.[17] Anisotropic temperature factors and corrections for anomalous dispersion effects were employed for the platinum atoms and isotropic temperature factors for all other atoms. A difference Fourier map then showed the hydrogen atom positions. These atoms were assigned isotropic temperature factors equal to 1.5 Å$^2$ plus the temperature factors of the atoms to which they were attached. Hydrogen atom contributions were included in subsequent cycles of least-squares refinement but no attempt was made to refine their positional or thermal parameters. The value for $R_1$ was 0.068 at this stage.

The elemental analysis had suggested the presence of one water molecule per unit cell.[15] Examination of a difference Fourier map revealed an unaccounted peak near the half nitrate anion and also disordered about the inversion center at (0, ½, 0). An oxygen atom with half occupancy was placed at the coordinates of this peak; the hydrogen atoms were not located.

Refinement was then continued using the new data set and the positional parameters and isotropic temperature factors from the previous refinement. After several cycles of refinement, using anisotropic temperature factors for the platinum atoms and isotropic temperature factors for all other atoms, $R_1$ was 0.050. The inclusion of redetermined fixed hydrogen atom parameters and anisotropic temperature factors for all nonhydrogen atoms resulted in a final $R_1$ value of 0.045. The final values for the weighted discrepancy index, $R_2 = [\Sigma w(|F_o| - |F_c|)^2/\Sigma w|F_o|^2]^{1/2}$, and the error in an observation of unit weight, $[\Sigma w(|F_o| - |F_c|)^2/(NO - NV)]^{1/2}$ where NO = 4421 independent observations and NV = 298 variables, were 0.058 and 1.96, respectively. No parameter changed by more than 0.073 of its error during the final cycle of refinement. Inspection of the function $\Sigma w\Delta^2$ for reflections ordered according to $|F_o|$ and (sin $\theta/\lambda$) showed satisfactory consistency.

A final difference Fourier map revealed (with either data set) several large positive and negative peaks ~1 Å on either side of each platinum atom with electron density about half that of a nitrogen atom (or ~5% that of a platinum atom). Attempts to refine the structure in the acentric space group $P1$ did not eliminate these features and generally resulted in poorer geometry. The extra peaks are probably the result of an inadequate absorption correction. An alternative explanation, namely, that the structure is slightly disordered along the direction of the $c$ axis, was briefly explored. A model in which platinum atoms with 0.05 occupancy were placed at the positions showing residual electron density and isotropically refined eliminated the peaks from the difference Fourier map and produced a platinum chain with satisfactory bond lengths and angles. Since this model did not significantly alter the parameters of the other atoms, and hence the structure, it was not used for the final refinement.

The final nonhydrogen atomic positional and thermal parameters together with their standard deviations are reported in Table II. The hydrogen atom positional and temperature factors are listed in Table III. The interatomic distances and angles are contained with their standard deviations in Table IV. The details of the hydrogen bonding observed in the crystal are given in Table V. A listing of the final observed and calculated structure factor amplitudes, the root mean square amplitudes of thermal vibration, and best planes calculations are available as Tables S1-S3, respectively.[18] The geometry of the $[(NH_3)_4Pt_2(C_5H_4NO)_2]_2^{5+}$ cation and the atom labeling scheme are given in Figure 1. Figure 2 portrays the unit cell packing diagram.

**Magnetic Susceptibility Measurements.** The magnetic susceptibility of the crystalline complex was measured at Bell Laboratories using an electronic Faraday balance over a temperature range of 4.4–280 K as described previously.[19] A small amount of ferromagnetic impurity was found in the sample on variation of the applied field at several temperatures. The magnetic susceptibility data were corrected for this impurity by extrapolation to infinite field (saturating conditions for the ferromagnetism) and subtraction of the additional measured susceptibility above this value from all data. The temperature-independent paramagnetism of the compound was obtained from the intercept of the plot of susceptibility, corrected for di-

**Table III.** Final Hydrogen Atom Positional Parameters (×10³) and Isotropic Thermal Parameters (Å²)[a]

| atom | *x* | *y* | *z* | *B* |
|---|---|---|---|---|
| H1 | 220 | −400 | −490 | 4.4 |
| H2 | 115 | −360 | −405 | 4.4 |
| H3 | 217 | −485 | −392 | 4.4 |
| H4 | 250 | −470 | −135 | 4.4 |
| H5 | 365 | −480 | −53 | 4.4 |
| H6 | 381 | −535 | −195 | 4.4 |
| H7 | −132 | −140 | −90 | 4.4 |
| H8 | −40 | −290 | −140 | 4.4 |
| H9 | −40 | −220 | −250 | 4.4 |
| H10 | 34 | −118 | 185 | 4.4 |
| H11 | 82 | −261 | 94 | 4.4 |
| H12 | 188 | −187 | 150 | 4.4 |
| H13 | 95 | 61 | −441 | 4.8 |
| H14 | 284 | 25 | −588 | 5.2 |
| H15 | 485 | −137 | −573 | 4.9 |
| H16 | 496 | −263 | −411 | 4.1 |
| H23 | 412 | 37 | 195 | 4.2 |
| H24 | 639 | −78 | 210 | 4.8 |
| H25 | 729 | −286 | 63 | 5.1 |
| H26 | 591 | −379 | −117 | 4.4 |

[a] Hydrogens are labeled according to the following scheme: H1–H12 are ammine hydrogens, with H1–H3 on N1, H4–H6 on N2, etc.; the others are labeled according to the carbon atoms to which they are attached.

amagnetism, vs. $1/(T-\theta)$. The value was determined to be $676 \times 10^{-6}$ cm³ g-atom$^{-1}$.

The magnetic susceptibility, corrected for underlying diamagnetism and temperature-independent paramagnetism, of solid *cis*-diammineplatinum α-pyridone blue per tetranuclear platinum unit, $\chi_T'$, at various temperatures is given in Table S4. A plot of $\chi_T'$ vs. $T$ may be seen in Figure 3. The dependence of $\chi_T'$ on temperature fits a Curie–Weiss expression, $\chi_T' = C_T/(T-\theta)$, where $\theta = -0.01$ K (solid curve in Figure 3). From the Curie constant, 0.4109 ± 0.0008 cm³ g-atom$^{-1}$ K$^{-1}$, the effective magnetic moment ($\mu_{eff} = 2.8273(C_T)^{1/2}$) was determined to be 1.81 $\mu_B$. This value is consistent with the presence of one unpaired electron arising, formally, from the presence of three diamagnetic square Pt(II) ($d^8$) and one paramagnetic platinum(III) ($d^7$) ion per tetranuclear platinum unit. The low value of the Weiss constant implies that there is little interionic magnetic interaction in the crystal lattice.

**Single Crystal ESR Measurements.** Three crystals of *cis*-diammineplatinum α-pyridone blue were mounted on quartz rods along three mutually orthogonal coordinate axes. The directions between the magnetic field and these axes were varied systematically by rotating the quartz rod in the microwave cavity. The coordinate axes were defined to be the long ($a$) axis of the crystal, $Z_{xtal}$ (intersection of the (010) and (001) faces), the vector orthogonal to this axis in the plane of the (010) face, $Y_{xtal}$ ($b^*Xa$), and the vector normal to the (010) face, $X_{xtal}$ ($b^*$). Spectra were recorded using a Varian E-line ESR spectrometer with single-crystal goniometer and variable-temperature accessories. The microwave frequency was determined using diphenylpicrylhydrazyl (DDPH) as a standard. The measured temperature was 163 K.

Only one ESR transition was observed at any given orientation of the crystal relative to the applied magnetic field. The resonant field position of this signal varied as the crystal was rotated. The signal also changed by ~20% of its intensity on rotation, as expected from the anisometric crystal dimensions. Two of the three crystals also showed additional peaks which varied on rotation; their intensities were less than 8% that of the main resonance. The extra peaks probably arise from fragments of *cis*-diammineplatinum α-pyridone blue that became attached to the rod or crystal during mounting.

Effective $g^2$ values ($g^2_{eff}$) corresponding to the single transition observed were determined as a function of $\theta$, the angle between the magnetic field and each of the three orthogonal coordinate axes. The results are presented in Figure 4. Spectra can be described by the following spin Hamiltonian:

$$\hat{\mathcal{H}} = \beta \hat{\mathbf{S}} \cdot \mathbf{g} \cdot \mathbf{H} \qquad (1)$$

**Table IV.** Interatomic Distances (Å) and Angles (deg)[a]

| | | | |
|---|---|---|---|
| | Coordination Sphere | | |
| Pt1–Pt2 | 2.7745 (4) | Pt2–Pt2′ | 2.8770 (5) |
| Pt1–N1 | 2.016 (8) | Pt2–N3 | 2.024 (8) |
| Pt1–N2 | 2.041 (7) | Pt2–N4 | 2.026 (8) |
| Pt1–N11 | 2.033 (7) | Pt2–O12 | 2.022 (6) |
| Pt1–N21 | 2.018 (7) | Pt2–O22 | 2.016 (6) |
| Pt1–O3 | 3.321 (9) | | |
| Pt1–Pt2–Pt2′ | 164.60 (2) | Pt2–Pt1–O3 | 167.8 (2) |
| N1–Pt1–N2 | 89.2 (3) | N3–Pt2–N4 | 91.1 (4) |
| N1–Pt1–N11 | 88.9 (3) | N3–Pt2–O12 | 88.0 (3) |
| N1–Pt1–N21 | 176.1 (3) | N3–Pt2–O22 | 178.3 (5) |
| N2–Pt1–N11 | 174.7 (3) | N4–Pt2–O12 | 178.4 (3) |
| N2–Pt1–N21 | 91.6 (3) | N4–Pt2–O22 | 88.5 (3) |
| N11–Pt1–N21 | 89.9 (3) | O12–Pt2–O22 | 92.4 (3) |
| | Pyridonate Rings | | |
| O12–C12 | 1.32 (1) | O22–C22 | 1.29 (1) |
| N11–C12 | 1.33 (1) | N21–C22 | 1.35 (1) |
| C12–C13 | 1.40 (1) | C22–C23 | 1.43 (1) |
| C13–C14 | 1.37 (1) | C23–C24 | 1.36 (1) |
| C14–C15 | 1.40 (2) | C24–C25 | 1.40 (2) |
| C15–C16 | 1.37 (1) | C25–C26 | 1.36 (1) |
| C16–N11 | 1.36 (1) | C26–N21 | 1.37 (1) |
| Pt1–N11–C12 | 123.0 (6) | Pt1–N21–C22 | 123.0 (6) |
| Pt1–N11–C16 | 115.5 (6) | Pt1–N21–C26 | 118.8 (6) |
| Pt2–O12–C12 | 122.8 (5) | Pt2–O22–C22 | 123.0 (6) |
| C12–N11–C16 | 120.7 (8) | C22–N21–C26 | 118.0 (8) |
| O12–C12–N11 | 120.9 (8) | O22–C22–N21 | 121.2 (8) |
| O12–C12–C13 | 118.0 (8) | O22–C22–C23 | 117.8 (8) |
| N11–C12–C13 | 121.1 (9) | N21–C22–C23 | 121.1 (8) |
| C12–C13–C14 | 118.4 (9) | C22–C23–C24 | 118.9 (9) |
| C13–C14–C15 | 120.3 (9) | C23–C24–C25 | 119.6 (9) |
| C14–C15–C16 | 118.5 (9) | C24–C25–C26 | 118.9 (9) |
| C15–C16–N11 | 120.8 (9) | C25–C26–N21 | 123.4 (9) |
| | Nitrate Anions | | |
| N7–O3 | 1.24 (1) | N8–O6 | 1.28 (2) |
| N7–O4 | 1.26 (1) | N8–O7 | 1.11 (2) |
| N7–O5 | 1.22 (1) | N8–O8 | 1.25 (3) |
| N9–O9 | 1.14 (5) | N9–O10 | 1.18 (5) |
| N9–O11 | 1.26 (4) | | |
| O3–N7–O4 | 119.2 (10) | O6–N8–O7 | 130 (3) |
| O3–N7–O5 | 120.9 (9) | O6–N8–O8 | 113 (2) |
| O4–N7–O5 | 120.0 (9) | O7–N8–O8 | 116 (3) |
| O9–N9–O10 | 118 (4) | O9–N9–O11 | 127 (4) |
| | | O10–N9–O11 | 115 (4) |

[a] See footnotes *a* and *b*, Table II; primed atoms are related to the unprimed ones by an inversion center at the origin. Values were not corrected for thermal motion.

where $\beta$ is the Bohr magneton, $\hat{\mathbf{S}}$ is the spin operator ($S = \frac{1}{2}$), $\mathbf{g}$ is the anisotropic $\mathbf{g}$ tensor, and $\mathbf{H}$ is the resonant field vector. Elements of the $\mathbf{g}^2_{eff}$ tensor in the crystal coordinate axis system[20] were determined by least-squares refinement in the following manner. Data from each of the three crystal axis mountings were used to obtain two diagonal and one off-diagonal elements. The diagonal elements were then set equal to their average value and the off-diagonal elements were refined again using the three data sets. The results in the laboratory frame are

$$g^2_{eff} = \begin{vmatrix} 4.677 & -0.572 & 0.831 \\ -0.572 & 5.469 & -0.0087 \\ 0.831 & -0.0087 & 5.105 \end{vmatrix} \qquad (2)$$

Calculated curves are shown as solid lines with the experimental data in Figure 4. The $\mathbf{g}^2_{eff}$ tensor was then diagonalized, resulting in the following principal components of the $\mathbf{g}$ tensor of *cis*-diammineplatinum α-pyridone blue:

$$g_{xx} = 2.307; g_{yy} = 2.455; g_{zz} = 1.975 \qquad (3)$$

No hyperfine interactions were observed in the single-crystal spectra.

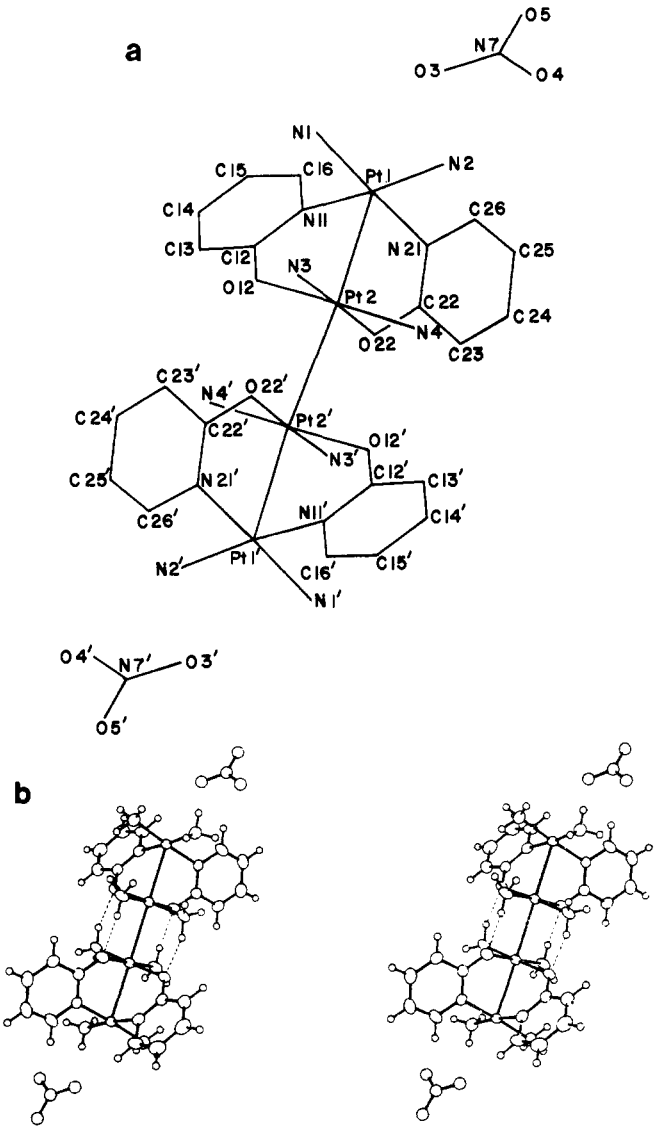


**Figure 1.** Geometry of the *cis*-diammineplatinum $\alpha$-pyridone blue cation and capping nitrate anions showing (a) the atom labeling scheme and (b) a stereoscopic view with 40% probability thermal ellipsoids. The four intracation hydrogen bonds are represented by dashed lines. For clarity, thermal parameters of the capping nitrate atoms were set equal to 3.0 Å$^2$ and those of the hydrogen atoms to 1.0 Å$^2$.

Since the X-ray crystal structure of the compound is known (vide supra), it was a straightforward matter to relate the $g$ values of eq 3 to the geometry of the tetranuclear cation. Atomic positions were first transformed from triclinic coordinates (Table II) to those of the crystal, $X_{xtal}$, $Y_{xtal}$, and $Z_{xtal}$, and then to those of the principal axes of the **g** tensor. The vector along the $Pt_4$ chain passing through the crystallographic inversion center intersects $g_{zz}$ at an angle of 1.1°. The $g_{xx}$ and $g_{yy}$ components do not lie along the Pt–N and Pt–O bonds, but rather subtend angles ranging from 16.3 to 33.8° (plus their complements) with these vectors, the average value being 27.4° (Table S5).[18]

## Discussion

**Description of the Structure. The Tetranuclear Cation.** The $[(NH_3)_4Pt_2(C_5H_4NO)_2]_2^{5+}$ cation consists of a tetranuclear chain of platinum atoms linked through amidate bridges, hydrogen bonds, and partial metal–metal bonding (Figure 1). The two dimers comprising the tetrameric chain are related through a crystallographically required inversion center. Each dimer consists of two *cis*-diammineplatinum units bridged by two $\alpha$-pyridonate ligands. Within a dimer, the Pt(1)–Pt(2) bond distance is 2.7745 (4) Å. The coordination sphere of the outer platinum atom is composed of two ammine ligands and

Table V. Hydrogen-Bonding Interactions[a]

| D | H | A[b] | D–H, Å | H···A, Å | D···A, Å | ∠D–H···A, deg |
|---|---|---|---|---|---|---|
| N1 | H1 | O5 (I) | 0.90 | 2.14 | 2.99 | 158 |
| N1 | H2 | O6 | 0.98 | 2.16 | 3.11 | 166 |
| N1 | H3 | O7 (II) | 0.93 | 2.12 | 3.04 | 174 |
| N2 | H4 | O11 (III) | 0.86 | 2.12 | 2.93 | 157 |
| N2 | H5 | O4 (IV) | 0.92 | 2.26 | 2.97 | 134 |
| N2 | H6 | O4 | 0.89 | 2.45 | 3.09 | 129 |
| N3 | H7 | O22 (V) | 0.91 | 1.99 | 2.81 | 152 |
| N3 | H8 | O11 (III)[c] | 1.01 | 2.10 | 3.03 | 153 |
| N3 | H8 | OW1[c] | 1.01 | 2.22 | 3.03 | 136 |
| N3 | H9 | O6 | 0.97 | 2.06 | 2.96 | 154 |
| N4 | H10 | O12 (V) | 0.97 | 1.97 | 2.82 | 146 |
| N4 | H11 | O10[c] | 0.96 | 2.07 | 2.96 | 152 |
| N4 | H11 | O11 (III)[c] | 0.96 | 2.13 | 3.02 | 154 |
| N4 | H12 | O4 (IV) | 0.93 | 2.36 | 3.10 | 137 |
| | | Other Proposed Hydrogen Bonds | | | | |
| OW1 | *d* | O7 (II) | | | 2.99 | |
| OW1 | *d* | O5 (VI) | | | 3.30 | |

[a] D, donor; A, acceptor. [b] Roman numerals indicate translation of the acceptor atom coordinates from the positions of Table II as follows: I, $(1-x), (-1-y), (-1-z)$; II, $(-x), (-1-y), (-1-z)$; III, $(-x), (-1-y), (-z)$; IV, $(1-x), (-1-y), (-z)$; V, $(-x), (-y), (-z)$; VI, $(-1+x), y, z$. [c] Owing to the disorder either O11 or OW1 (the lattice water) is present, not both; the same applies to the O10/O11 pair. [d] Not located.

the two deprotonated ring nitrogen atoms of the $\alpha$-pyridonate ligand. The inner platinum coordination sphere contains the two exocyclic oxygen atoms of the $\alpha$-pyridonate groups in addition to two ammines. The platinum coordination planes are tilted by 27.4° with respect to one another and, in addition, are twisted by 22° about the platinum–platinum bond axis. This geometry differs appreciably from that of the extensively studied one-dimensional conducting platinum chain complexes[5] where the platinum coordination planes are stacked in a parallel fashion. Unlike *cis*-diammineplatinum $\alpha$-pyridone blue, these one-dimensional complexes are not linked by bridging ligands. The bite distance of the $\alpha$-pyridonate ligand is 2.30 (1) Å and may be one factor contributing to the canting of the coordination planes. If so, then the failure of *trans*-diammineplatinum complexes to form analogous blue products is easily rationalized. It would be impossible to cant the planes to accommodate a doubly bridged trans structure. Another likely reason for the splaying and twisting of the coordination planes is the need to produce nonbonded $NH_3\cdots NH_3$ contacts of 3.67 Å, a value approximately equal to the sum of the van der Waals radii of the ammine groups. This steric interaction precludes the formation of doubly bridged blue platinum complexes having either a trans configuration or cis-oriented bulky amine ligands.

Linkage of the two dimeric units is achieved by a Pt(2)–Pt(2′) bond of 2.8770 (5) Å as well as four intrachain hydrogen bonds between the coordinated ammines of one dimer and the pyridonate oxygen atoms of the neighboring dimer (Figure 1). The resultant tetranuclear platinum cation is capped at both ends by a nitrate anion; the Pt–O3 distance is 3.321 (9) Å. The Pt(1)–Pt(2)–Pt(2′) angle within the zigzag chain is 164.60 (2)°. Comparable angles in the one-dimensional platinum chain compounds are 173.08 and 177.8° in $K_{1.75}Pt(CN)_4\cdot 1.5H_2O$[21] and $K_{1.6}Pt(C_2O_4)_2\cdot 1.2H_2O$,[22] respectively.

The cationic platinum oligomer is surrounded by nitrate anions and water molecules in the lattice (Figure 2). Two and one-half nitrate ions and a half water molecule occur in the asymmetric unit, leading to an average platinum formal oxidation state of 2.25 and a chemical formula of $[Pt_2(NH_3)_4(C_5H_4NO)_2]_2(NO_3)_5\cdot H_2O$.

Studies of one-dimensional metal chain complexes have

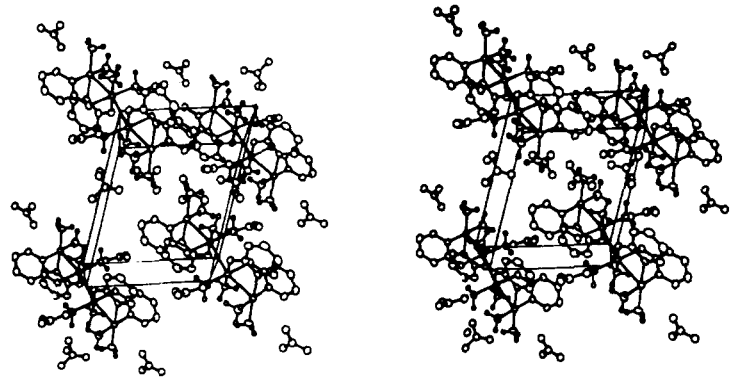

**Figure 2.** Stereoscopic view of the crystal packing showing the contents of four unit cells.

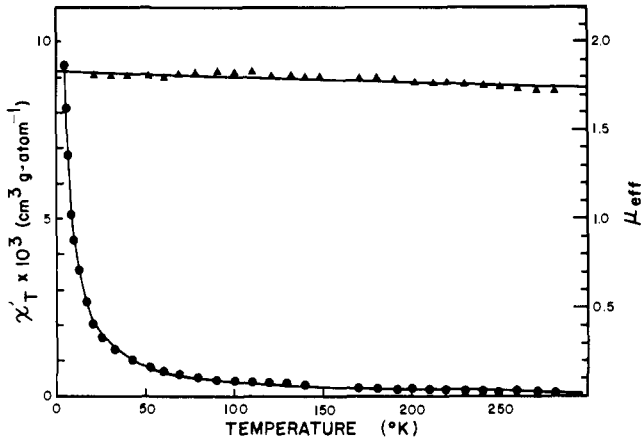


**Figure 3.** Temperature dependence of the magnetic susceptibility (●), $\chi_T'$, and effective magnetic moment (▲), $\mu_{eff}$, per tetrameric unit of *cis*-diammineplatinum α-pyridone blue. Experimental data have been corrected for diamagnetism and temperature-independent paramagnetism. Solid lines show the best least-squares fit to a Curie–Weiss law (see text) for 82 data points (Table S4), not all of which are depicted here.

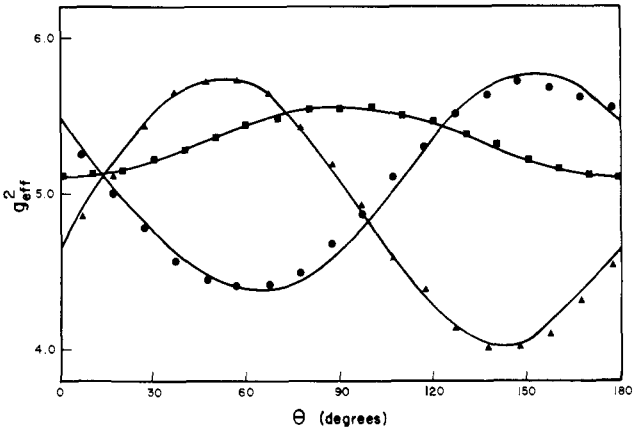


**Figure 4.** Angular variations of $g^2_{eff}$ for each of the three crystal axis mountings of *cis*-diammineplatinum α-pyridone blue. θ corresponds to the angle between the applied magnetic field and $X_{xtal}$ (▲), $Y_{xtal}$ (●), or $Z_{xtal}$ (■) for rotation about $Y_{xtal}$, $Z_{xtal}$, or $X_{xtal}$, respectively. The axes are defined in the text. Curves calculated by least-squares refinement of the data are given by the solid lines.

shown the metal–metal bond distance to be correlated with the formal oxidation state of the metal.[23] A similar correlation occurs for platinum compounds having bridging ligands. The platinum–platinum bond distances of 2.7745 and 2.8770 Å observed in *cis*-diammineplatinum α-pyridone blue (formal oxidation state 2.25) are intermediate between those found in bridged platinum(II) and platinum(III) complexes. The Pt(II)–Pt(II) distances are 3.229 and 3.11 Å in the *cis*-diammineplatinum(II) pyrophosphate dimer[24] and 2.95 Å in a *cis*-diammineplatinum(II) 1-methylthyminato dimer,[25] while the Pt(III)–Pt(III) bond distance is 2.466 Å in the sulfate bridged dimer $K_2[Pt_2(SO_4)_4(H_2O)_2]$.[26] These values are all somewhat shorter than the distances in one-dimensional platinum chain compounds having the same formal oxidation states.[23] This result might be due to the presence of bridging ligands; thus, within the structure of *cis*-diammineplatinum α-pyridone blue the bridged (Pt1–Pt2) bond is 0.1 Å shorter than the nonbridged value. In any event, the mean metal–metal bond distance observed in *cis*-diammineplatinum α-pyridone blue is consistent with the formally nonintegral platinum oxidation state of 2.25.

The Pt–O and Pt–N bond lengths within the coordination spheres of each of the two crystallographically independent platinum atoms do not differ significantly (Table IV). The minimum and maximum values are 2.016 (8) and 2.040 (7) Å, respectively, and the average is 2.025 Å. The geometry of the two independent pyridonate rings compares closely with that found for the four bridging pyridonate ligands in $Cr_2(mhp)_4$[27] (where mhp = 2-hydroxy-6-methylpyridinate). As expected, the pyridonate rings are planar (see Table S3), with the exocyclic oxygen atoms lying in the planes. The coordination sphere of each platinum is also planar, the two platinum atoms being displaced by 0.08 and 0.03 Å out of the plane toward one another.

**Anion Geometry, Hydrogen Bonding, and Crystal Packing.** The bond lengths and angles in the capping nitrate anion are normal. The other nitrate ions show greater geometric deviations that have no chemical significance in view of the fairly large standard deviations (Table IV). The capping and half-nitrate anions are planar while the nitrogen atom of the remaining nitrate group lies 0.06 Å out of the plane defined by the three oxygen atoms. The lack of planarity, high standard deviations in bond lengths and angles, as well as the high thermal parameters of this nitrate group suggest that it is partially disordered.

Hydrogen bonding plays an important role in stabilizing both the tetranuclear cation and the crystal lattice. Four intramolecular hydrogen bonds bridge the two *cis*-diammineplatinum dimers across the center of symmetry (Figures 1 and 2). These hydrogen bonds occur between the ammine hydrogen and pyridonate oxygen atoms and reinforce the central metal–metal bond. From the average N–H···O angle of 149°, we estimate each hydrogen bond to contribute at least 3 kcal/mol (or 12 kcal/mol altogether) to the stabilization of the tetranuclear cation. The failure of *cis*-dichloroplatinum reagents having bulky, non-hydrogen-bonding ligands to form blue products is noteworthy in this context.

A stereoview of the unit cell packing is shown in Figure 2. The lattice is composed of hydrophobic and, predominantly, hydrophilic centers. Limited pairwise stacking interaction

occurs between pyridonate rings of neighboring cations. Nitrate anions and water molecules are interposed between the cations and there are extensive hydrogen-bonding interactions. The details of the hydrogen-bonding network are given in Table V and Figure 2.

**Magnetic Susceptibility.** The bulk magnetic susceptibility results show that *cis*-diammineplatinum α-pyridone blue is a simple Curie paramagnet. Discrete paramagnetic platinum complexes are quite rare and include examples such as the $NO^+$ and $O_2^+$ salts of the $[PtF_6]^-$ ion, $\mu_{eff} = 1.74\ \mu_B$,[28] and tetra-*n*-butylammonium bis(maleonitriledithiolato)platinate(III).[29] The value of 1.81 $\mu_B$ for the effective magnetic moment of the $[Pt_2(NH_3)_4(C_5H_4NO)_2]_2^{5+}$ cation indicates the presence of one unpaired electron. This electron is presumably delocalized over the $Pt_4$ chain since X-ray photoelectron spectroscopic studies showed only one set of platinum 4f binding energies.[16] The moment is slightly higher than the value of 1.73 $\mu_B$ calculated from the spin-only formula, consistent with the existence of spin-orbit coupling.

The small value of the Weiss constant shows that there are no long-range exchange interactions in the solid state. This result is not surprising in view of the crystal lattice packing (Figure 2). The tetranuclear cation is loosely capped at both ends by nitrate anions. Moreover, since the axis of the oligomer does not lie along a unit cell edge, neighboring cations are displaced from one another rather than forming an infinite chain. Nitrate ions separate the chains in the lateral directions. Unlike the columnar stacked tetracyanoplatinate salts, *cis*-diammineplatinum α-pyridone blue is not expected to have interesting conductivity properties, and none are observed.[30]

**Single-Crystal Electron Spin Resonance.** The magnitudes of the principal components of the **g** tensor (eq 3) are similar to those obtained for the one-dimensional chain compound, $K_2Pt(CN)_4Br_{1/3}\cdot 3H_2O$,[31] having $g_\parallel = 1.946$ (5) and $g_\perp = 2.336$ (5), and for Pt(IV) doped Magnus' green salt, $[Pt(NH_3)_4][PtCl_4]$,[32] where $g_\parallel = 1.939$ (2) and $g_\perp = 2.504$ (2). As for these materials, the measured **g** values for *cis*-diammineplatinum α-pyridone blue are described by a $d_{z^2}$ hole state ($z$ taken along the mean $Pt_4$ chain axis) with an admixture of lower lying $d_{xz}$, $d_{yz}$ states due to spin-orbit coupling.[33] Assignment to a state of different symmetry, e.g., $p_z$ where (according to crystal field arguments[34]) $g_\parallel = 2 > g_\perp$, or $d_{x^2-y^2}$ where $g_\parallel > g_\perp > 2$, would not be consistent with the observed results. Moreover, a $d_{z^2}$ assignment is consistent with the orientation of $g_\parallel$ along the mean $Pt_4$ chain axis.

The decrease in the values of $g_\perp$ along the series Pt(IV) doped $[Pt(NH_3)_4][PtCl_4]$, *cis*-diammineplatinum α-pyridone blue, and $K_2Pt(CN)_4Br_{1/3}\cdot 3H_2O$ most likely represents an increase in the degree of delocalization of the unpaired spin. Using crystal field theory with second-order perturbation terms of the equation

$$g_\perp = 2N^2 + 6N(\xi/\Delta E) - 6N^2(\xi/\Delta E)^2$$
$$g_\parallel = 2N^2 - 3N^2(\xi/\Delta E)^2 \qquad (4)$$

where $N$ is the normalization coefficient for the zero-order wave function arising from the spin-orbit interaction, $\xi$ is the spin-orbit coupling constant, and $\Delta E$ is the average energy separation between the $d_{z^2}$ and $d_{xz}$, $d_{yz}$ states, gives $N = 0.997$ and $\xi/\Delta E = 0.071$ for *cis*-diammineplatinum α-pyridone blue. These may be compared with the values of $N = 0.99$, $(\xi/\Delta E) = 0.068$, and $N = 0.99$, $\xi/\Delta E = 0.10$ in $K_2Pt(CN)_4Br_{1/3}\cdot 3H_2O$ and Pt(IV) doped $[Pt(NH_3)_4][Pt(CN)_4]$, respectively. These results reflect increased $d_{z^2}$ character, less mixing with $d_{xz}$, $d_{yz}$ states, and increased energy level separation ($\Delta E$) along this series.

In contrast to the Pt(IV) doped Magnus' green salt, *cis*-diammineplatinum α-pyridone blue and the partially oxidized tetracyanoplatinate complex show no ESR hyperfine interactions in the solid state. This result is not surprising given the relatively high unpaired spin densities, and therefore magnetic moments, in these complexes as compared to the dilute spin system of the doped Magnus' green salt. Aqueous solution ESR spectra of the α-pyridone blue, the only one of the three that maintains its oligomeric structure in solution, do show $^{195}Pt$ hyperfine coupling interactions, reflecting the delocalization of the unpaired electron along the platinum chain through the $d_{z^2}$-like molecular orbitals.[12]

**Relationship to Blue and Other Platinum Complexes.** The molecular structure of *cis*-diammineplatinum α-pyridone blue embodies features characteristic of all blue platinum complexes. X-ray photoelectron spectra of various blues have established that they have nearly identical electronic structures.[16] An EXAFS (extended X-ray absorption fine structure) study of *cis*-diammineplatinum uridine blue[35] has revealed short Pt-Pt bond distances ($r$ = 2.9 Å), comparable in length to those reported above. Solution chemical and spectroscopic studies[12] also show the α-pyridone blue to be a close analogue of others in the class.

Recently, the structure of a *cis*-diammineplatinum(II) 1-methylthymine dimer, isolated from the reaction mixture of the platinum 1-methylthymine blue, has been reported.[25] The geometry of this complex bears a close resemblance to that of *cis*-diammineplatinum α-pyridone blue. Two 1-methylthyminate ligands use their heterocyclic, deprotonated ring nitrogen, N3, and exocyclic oxygen, O4, atoms to bridge two *cis*-diammineplatinum units. In contrast to the α-pyridone blue, the ligands bridge in a head to tail fashion. The resulting metal-metal distance of 2.97 Å, while short for a binuclear platinum(II) complex, is significantly longer than in the partially oxidized α-pyridone blue. The characteristic splaying and twisting of coordination planes to accommodate the ammine-ammine repulsive interactions and the short bite distances of bridging ligands are observed in this thyminate complex. These features also occur in the structure of polymeric *cis*-diammineplatinum pyrophosphate, which is strikingly similar to that of *cis*-diammineplatinum α-pyridone blue (cf. ref 24). The splaying and twisting of the *cis*-diammineplatinum units, as well as hydrogen-bonding interactions between ammine ligands and exocyclic oxygen atoms, are geometric features that presumably occur in all *cis*-diammineplatinum oligomeric complexes.

Molecular weight studies[11,12] of platinum blues suggest that, in solution, long polymeric chains are formed. The doubly bridged arrangement of ligands in both the α-pyridone blue and the 1-methylthyminate dimer stereochemically prohibit long chain oligomerization. Elongation of the platinum chain of pyrimidine blues may, instead, be propagated through use of only one bridging ligand, with coordination to the platinum atom by, in the case of the uracilate anion, a mixture of N3 and O2 or N3 and O4 ligating atoms. A mixture of such species having varying chain lengths would be difficult to crystallize. It seems quite likely from the present and related[9-16] studies, however, that the characteristics of mixed valency, oligomerization, and bridging amidate ligands, features exhibited by *cis*-diammineplatinum α-pyridone blue, are shared by all blue platinum amide complexes.

**Possible Relevance to the Binding of *cis*-DDP to DNA.** The structural features of the α-pyridone blue may reflect aspects of the binding of the antitumor drug *cis*-DDP to DNA. One model based on the structure of *cis*-diammineplatinum α-pyridone blue has been proposed previously.[36] In this model, *cis*-diammineplatinum units are linked by neighboring guanine bases on the polynucleotide chain through the deprotonated ring nitrogen, N1, and exocyclic oxygen, O6, atoms. A green platinum-hypoxanthine complex has been isolated[12] and the hypoxanthine anion may bridge neighboring *cis*-diammineplatinum units in this fashion. EXAFS results,[37] however, demonstrate that no short platinum-platinum bonding inter-

actions are present in reaction mixtures obtained by incubation of *cis*-DDP with calf thymus DNA. The structures of *cis*-diammineplatinum α-pyridone blue, the *cis*-diammineplatinum(II) 1-methylthyminate complex, described above, and a 1-methylcytosine silver dimer[38] (where cytosine anions bridge silver atoms through N3 and O4) having no metal-metal interaction all serve as examples of the coordination of an exocyclic oxygen atom to soft transition metals. Similar binding modes, involving coordination to the metal through an exocyclic keto oxygen atom, may therefore be involved in the binding of *cis*-DDP to DNA.

**Acknowledgments.** This work was supported at Columbia University by National Institutes of Health Grant CA-15826 and by a National Research Service Award (to D.J.S.), CA-05806, both from the National Cancer Institute. A generous loan of $K_2PtCl_4$ from Engelhard Industries is gratefully acknowledged. We also thank Drs. P. W. R. Corfield and F. J. DiSalvo for advice, Dr. L. V. Interrante for obtaining powder conductivity data, and A. Evans of Varian Associates for experimental assistance.

**Supplementary Material Available:** Tables (S1-S5) of the final observed and calculated structure factor amplitudes, the root mean square amplitudes of thermal vibration, best planes, the magnetic relative susceptibility of solid *cis*-diammineplatinum α-pyridone blue, and orientation of $g$ components and bond vectors (33 pages). Ordering information is given on any current masthead page.

## References and Notes

(1) (a) Columbia University; (b) Bell Laboratories.
(2) National Science Foundation Predoctoral Fellow, 1975-1978.
(3) K. A. Hofmann and G. Bugge, *Chem. Ber.*, **41**, 312 (1908).
(4) R. D. Gillard and G. Wilkinson, *J. Chem. Soc.*, 2835 (1964).
(5) For a review see J. S. Miller and A. J. Epstein, *Prog. Inorg. Chem.*, **20**, 113 (1976).
(6) D. B. Brown, R. D. Burbank, and M. B. Robin, *J. Am. Chem. Soc.*, **90**, 5621 (1968); **91**, 2895 (1969), and references cited therein.
(7) B. Rosenberg, L. Van Camp, J. E. Trosko, and V. H. Mansour, *Nature (London)*, **222**, 385 (1969); B. Rosenberg and L. Van Camp, *Cancer Res.*, **30**, 1799 (1970). For a review see J. M. Hill, E. Loeb, A. MacLellan, N. O. Hill, A. Khan, and J. J. King, *Cancer Chemother. Rep.*, **59**, 647 (1975).
(8) P. J. Davidson, P. J. Faber, R. G. Fischer, Jr., S. Mansy, H. J. Peresie, B. Rosenberg, and L. Van Camp, *Cancer Chemother. Rep.*, **59**, 287 (1975); R. J. Speer, H. Ridgeway, L. M. Hall, D. P. Stewart, K. E. Howe, D. Z. Lieberman, A. D. Newman, and J. M. Hill, *ibid.*, **59**, 629 (1975).
(9) E. I. Lerner, Ph.D. Dissertation, Columbia University, 1976.
(10) C. M. Flynn, Jr., T. S. Viswanathan, and R. B. Martin, *J. Inorg. Nucl. Chem.*, **39**, 437 (1977).
(11) A. J. Thomson, I. A. G. Roos, and R. D. Graham, *J. Clin. Hematol. Oncol.*, 7, 242 (1977).
(12) E. I. Lerner, J. K. Barton, W. R. Bauer, and S. J. Lippard, to be submitted for publication.
(13) B. Lippert, *J. Clin. Hematol. Oncol.*, 7, 26 (1977).
(14) R. D. Macfarlane and D. F. Torgerson, *Science*, **191**, 920 (1976).
(15) J. K. Barton, H. N. Rabinowitz, D. J. Szalda, and S. J. Lippard, *J. Am. Chem. Soc.*, **99**, 2827 (1977).
(16) J. K. Barton, S. A. Best, S. J. Lippard, and R. A. Walton, *J. Am. Chem. Soc.*, **100**, 3785 (1978).
(17) (a) Scattering factors for the neutral, nonhydrogen atoms were taken from "International Tables for X-ray Crystallography", Vol. IV, Kynoch Press, Birmingham, England, 1974, p 72 ff. Hydrogen atom scattering factors were those of R. F. Stewart, E. R. Davidson, and W. T. Simpson, *J. Chem. Phys.*, **42**, 3175 (1965). (b) Anomalous scattering factors were those of D. T. Cromer and D. Liberman, *J. Chem. Phys.*, **53**, 1891 (1970).
(18) See paragraph at end of paper regarding supplementary material.
(19) A. P. Ginsberg, M. E. Lines, K. D. Karlin, S. J. Lippard, and F. D. DiSalvo, *J. Am. Chem. Soc.*, **98**, 6958 (1976).
(20) See, for example, J. E. Wertz and J. R. Bolton, "Electron Spin Resonance", McGraw-Hill, New York, 1972, p 135 ff.
(21) A. H. Reis, Jr., S. W. Peterson, D. M. Washecheck, and J. S. Miller, *J. Am. Chem. Soc.*, **98**, 234 (1976).
(22) A. H. Reis, Jr., S. W. Peterson, and S. C. Lin, *J. Am. Chem. Soc.*, **98**, 7839 (1976).
(23) (a) J. M. Williams, *Inorg. Nucl. Chem. Lett.*, **12**, 651 (1976). (b) A. H. Reis, Jr., and S. W. Peterson, *Inorg. Chem.*, **15**, 3186 (1976). (c) Similar correlations have been drawn between the metal-metal bond distance and bond order. The bond order, $p_{rs}$, for the r-s bond may be defined as $p_{rs} = \sum_j n_j c_{jr} c_{js}$ where $n_j$ is the number of electrons in the $j$th molecular orbital and $c_{jr}$, $c_{js}$ correspond to the atomic orbital coefficients used to form the $j$th molecular orbital. If the molecular orbitals in the α-pyridone blue are analogous to those obtained in an extended Hückel calculation for butadiene,[23d] with four electrons occupying two bonding orbitals and three electrons in two antibonding orbitals, we find $p_{12} = 0.223$ and $p_{22'} = 0.360$ for the outer and inner metal-metal bonds respectively. The average bond order would then be 0.269. (d) A. Streitwieser, Jr., "Molecular Orbital Theory for Organic Chemists", Wiley, New York, 1961, p 55.
(24) (a) J. A. Stanko, results quoted by M. J. Cleare in "Platinum Coordination Complexes in Chemotherapy", T. A. Connors and J. J. Roberts, Eds., Springer-Verlag, New York, 1974, pp 24-26; (b) J. A. Stanko, private communication.
(25) C. J. L. Lock, H. J. Peresie, B. Rosenberg, and G. Turner, *J. Am. Chem. Soc.*, **100**, 3371 (1978).
(26) G. S. Muraveiskaya, G. A. Kukina, V. S. Orlova, O. N. Evstaf'eva, and M. A. Porai-Koshits, *Dokl. Akad. Nauk. SSSR*, **226**, 596 (1976).
(27) F. A. Cotton, P. E. Fanwick, R. H. Niswander, and J. C. Sekutowski, *J. Am. Chem. Soc.*, **100**, 4725 (1978).
(28) (a) N. Bartlett and D. H. Lohmann, *J. Chem. Soc.*, 5253 (1962); (b) N. Bartlett and S. P. Beaton, *Chem. Commun.*, 167 (1966).
(29) (a) A. Davison, N. Edelstein, R. H. Holm, and A. H. Maki, *J. Am. Chem. Soc.*, **85**, 2029 (1963); *Inorg. Chem.*, **3**, 814 (1964); (b) E. Billig, S. I. Shupack, J. H. Waters, R. Williams, and H. B. Gray, *J. Am. Chem. Soc.*, **86**, 926 (1964); (c) R. Kirmse, W. Dietzsch, and B. V. Solov'ev, *J. Inorg. Nucl. Chem.*, **39**, 1157 (1977).
(30) Dr. L. V. Interrante kindly measured the powder conductivity and found it to be $4 \times 10^{-8}\ \Omega^{-1}\ cm^{-1}$.
(31) F. Mehran and B. A. Scott, *Phys. Rev. Lett.*, **31**, 1347 (1973).
(32) F. Mehran and B. A. Scott, *Phys. Rev. Lett.*, **31**, 99 (1973).
(33) T. Krigas and M. T. Rogers, *J. Chem. Phys.*, **55**, 3035 (1971).
(34) B. Bleaney, K. D. Bowers, and M. H. L. Pryce, *Proc. R. Soc. London, Ser. A*, **228**, 166 (1955).
(35) B. K. Teo, K. Kijima, and R. Bau, *J. Am. Chem. Soc.*, **100**, 621 (1978).
(36) J. K. Barton and S. J. Lippard, *Ann. N.Y. Acad. Sci.*, **313**, 686 (1978).
(37) B. K. Teo, P. Eisenberger, J. Reed, J. K. Barton, and S. J. Lippard, *J. Am. Chem. Soc.*, **100**, 3225 (1978).
(38) L. G. Marzilli, T. J. Kistenmacher, and M. Rossi, *J. Am. Chem. Soc.*, **99**, 2797 (1977).